Am J Transl Res 2025;17(5):3307-3321
www.ajtr.org /ISSN:1943-8141/AJTR0163946

Original Article

Luteolin alleviates Herpes Simplex Keratitis by inhibiting inflammatory responses via suppressing the PTGS2/NF-κB signaling pathway

Xudong Zhao[1*], Zhichao Ren[2*], Dingwen Cao[1], Yusen Huang[1]

[1]*State Key Laboratory Cultivation Base, Shandong Provincial Key Laboratory of Ophthalmology, Shandong Eye Institute, Shandong First Medical University and Shandong Academy of Medical Sciences, Qingdao, Shandong, China;* [2]*Qingdao University, Qingdao Medical College, Qingdao, Shandong, China.* [*]*Equal contributors.*

Received February 15, 2025; Accepted April 23, 2025; Epub May 15, 2025; Published May 30, 2025

Abstract: Objective: Herpes Simplex Keratitis (HSK) is a leading cause of infectious-related blindness, primarily driven by corneal inflammation and dysregulated immune response. Luteolin (LUT), a flavonoid with anti-inflammatory and antiviral properties, has the potential to target key signaling pathways and provide therapeutic benefits. This study aimed to investigate the mechanisms through which LUT alleviates HSK. Methods: LUT's potential targets in HSK were identified using a systemic biology approach. Protein-Protein Interaction (PPI) analysis was performed to determine key hub genes. Molecular docking was used to assess LUT's binding affinity to PTGS2 and other key proteins. HSK mice were treated with LUT, and corneal opacity, edema, and thickness were then evaluated using slit-lamp microscopy and Optical Coherence Tomography. Inflammatory cytokine levels were quantified by quantitative Real-Time Polymerase Chain Reaction PCR (qRT-PCR), while PTGS2/NF-κB pathway activation, PTGS2 expression, and NF-κB phosphorylation levels were assessed by Western Blotting (WB). Results: LUT was found to regulate 30 HSK-related proteins, with AKT1, TNF, and PTGS2/NF-κB identified as key nodes. Furthermore, molecular docking confirmed a strong binding to PTGS2 (-9.7 kcal/mol). LUT treatment significantly reduced corneal opacity and edema, restoring corneal thickness to near-normal levels. RT-qPCR revealed downregulation of inflammatory cytokines, and WB analysis showed decreased PTGS2 expression and NF-κB phosphorylation, confirming LUT's role in attenuating corneal inflammation via inhibiting the PTGS2/NF-κB signaling pathway. Conclusions: LUT alleviates HSK by modulating the PTGS2/NF-κB signaling pathway, reducing inflammation and corneal damage, and highlighting its therapeutic potential for ocular inflammatory diseases.

Keywords: Herpes Simplex Keratitis, Traditional Chinese Medicine, LUT, PTGS2/NF-κB, inflammatory response

Introduction

Herpes Simplex Keratitis (HSK) is a severe ocular infection caused by Herpes Simplex Virus (HSV), often manifesting as dendritic ulcers and leading to corneal scarring, which can result in blindness [1-3]. HSK is the leading infectious cause of blindness in developed countries, affecting approximately 1.5 million people annually, with 40,000 cases potentially developing long-term visual impairment [4, 5]. Owing to its high risk of blindness, frequent recurrence, and potential for causing visual impairment, HSK is a major health concern, imposing significant physical, emotional, and economic burdens on both patients and society [6].

Current HSK interventions rely primarily on antiviral drugs, steroid therapy, and emerging immunomodulatory approaches. Despite their potential to reduce HSK duration and severity, these contemporary antiviral treatments have limitations, including the emergence of drug-resistant HSV strains [7] and inflammation-induced damage to corneal nerves [8]. Therefore, developing safe and effective novel treatments for repairing inflammation-damaged corneal nerve endings remains imperative [9].

Research has shown that the inflammatory process in HSK involves the activation of several signaling pathways, particularly the Prostaglandin-Endoperoxide Synthase 2 (PTGS2) and Nuclear Factor-kappa B (NF-κB) pathways

https://doi.org/10.62347/IQUZ8416

[10]. PTGS2, a pro-inflammatory enzyme involved in the host immune response, activates NF-κB, a transcription factor (TF) that regulates the expression of various inflammatory mediators. Upon activation, NF-κB translocates to the nucleus, where it induces the expression of multiple cytokines, chemokines, and adhesion molecules, thus perpetuating an inflammatory response.

Traditional Chinese Medicine (TCM), one of the world's oldest and most comprehensive medical systems, has shown unique efficacy in treating certain infectious diseases. Its holistic approach has led to the discovery of various natural compounds with significant anti-infective properties, such as artemisinin, quercetin, and curcumin [11, 12]. Although TCM has been widely employed in HSK treatment, the precise molecular mechanisms underlying its effects remain unclear. Luteolin (LUT), a flavonoid commonly found in various medicinal plants and herbs, exhibit notable anti-inflammatory and antioxidant properties and has shown potential in HSK treatment [13-15]. However, LUT's role in HSK treatment remains largely unexplored.

Herein, we investigated TCM prescriptions that may be used to treat HSK, identifying their active ingredients, target proteins, and related signaling pathways. Our *in vivo* and *in vitro* analyses revealed that LUT alleviated HSK by modulating the PTGS2/NF-κB pathway, providing novel insights and experimental evidence to support the modernization of TCM research.

Materials and methods

Data acquisition and processing

We searched various databases for literature published between January 1, 2000, and June 1, 2025, using the key phrases "Herpes Simplex Keratitis", "Viral Keratitis", "Traditional Chinese Medicine Treatment", and "Chinese Herbal Medicine Treatment". Details of the databases, software used, and inclusion criteria are provided in Supplementary Tables 1, and 2. After examining the TCM prescriptions and performing frequency analysis of their constituent drugs, the top 10 most common drugs were selected for further investigation. Relevant parameters and chemical components of these drugs were queried using the TCM Systems Pharmacology Database. Effective active ingredients were then screened based on the criteria of Oral Bioavailability (OB) ≥30% and Drug-Likeness (DL) ≥0.18. The targets associated with these active ingredients were compared to HSK targets using Venny software to identify potential therapeutic targets. The STRING database was used to construct a Protein-Protein Interaction (PPI) network, which was visualized using Cytoscape 3.6.1. The top 5 targets, ranked by degree, were identified as potential core targets for the active ingredients. Gene Ontology (GO) and Kyoto Encyclopedia of Genes and Genomes (KEGG) pathway enrichment analyses were further performed to identify key biological processes (BPs), cellular components (CCs), molecular functions (MFs), and pathways implicated in the therapeutic mechanisms.

The interactions between the active ingredients and their targets were further explored using molecular docking with AutoDock-Vina, evaluating the binding affinity between receptors and ligands retrieved from the PubChem and RCSB-PDB databases. Furthermore, docking results were visualized using PyMOL 2.4.1 to elucidate the structural basis of interactions between active ingredients and their targets. Detailed steps are outlined in Supplementary Table 3.

Animal study

Female Wild-Type (WT) C57BL/6 mice (6-8 weeks) with normal eye development were acquired from Beijing Vital River Laboratory Animal Technology Co., Ltd. (Beijing, China) and housed in a controlled environment (23°C; 55±5% humidity). All animal procedures adhered to the ARVO Statement and Shandong Eye Institute's guidelines for the use of animals in ophthalmic research. The study protocol was approved by the Animal Investigation Committee of Shandong First Medical University (Approval number: SDSYKYJS 20240416).

To ensure adequate pain relief, anesthesia was administered via intraperitoneal injection of 0.6% pentobarbital at a dosage of 0.25 mg-0.3 mg per mouse, based on body weight. Euthanasia was performed by cervical dislocation to ensure a rapid and painless death.

HSV-1 culture, amplification, and HSK model establishment

Herpes Simplex Virus Type 1 (HSV-1) was propagated in African green monkey kidney (Vero)

cells, and its titer was determined using the plaque assay. Briefly, the Vero cells were seeded in 24-well plates at a density of 1×10^5 cells/well. At 70-80% confluence, the cells were incubated with the virus solution. Following that, the virus solution was removed, and the cells were overlaid with a complex medium consisting of Dulbecco's Modified Eagle Medium (DMEM)-F12, 0.6% agar, and 2% Fetal Bovine Serum (FBS). Plaques were counted after incubation, and the virus titer was calculated as plaque-forming units per milliliter (pfu/mL).

For the HSK model, the corneal surface of the mice was scratched with a 30-G needle to create a crosshatch pattern consisting of 20 vertical and 20 horizontal scratches. The animals were then infected with the McKrae HSV-1 strain at a titer of 1×10^6 pfu [16].

Drugs

The stock solution of LUT (BL-20231106002; BOLIN Biotech Co., Ltd., Shaanxi, China) was prepared in a mixture containing 5% DMSO, 5% Tween-80, and 90% saline. The working solution was administered via subconjunctival injection at a volume of 5 μL per eye, with a dosing schedule of once every two days, starting from -1 day post-infection and continuing throughout the treatment period. A vehicle control solution containing the same proportions of DMSO and Tween-80 in saline was used for comparison.

To investigate the role of the NF-κB and PTGS2 signaling pathways in HSK, the working solution of BAY 11-7082 (40 mM; MedChem Express, Shanghai, China) was prepared by dissolving the powder in a mixture containing 10% DMSO and 70% saline solution. This solution was subconjunctivally administered at 5 μL per eye per day, starting from 2 days before infection and continuing through 1 day post-infection. For PTGS2 inhibition, FK 3311 (COX-2 Inhibitor V; 20 mM; MedChem Express) was similarly prepared by dissolving the powder in a mixture of 10% DMSO and 70% saline. This solution was also administered subconjunctivally at 5 μL per eye per day, starting from 2 days before infection and continuing through 1 day post-infection. The control group for both treatments received the same volume of vehicle solution, which consisted of 10% DMSO, 20% sulfobutylether-β-cyclodextrin (SBE-β-CD), and 70% saline.

HSK score

Keratitis severity was graded using a 0-4 scale. Notably, HSK scores of 0 indicated normal conditions without epithelial or punctate lesions, edema, or stromal opacity. A score of 1 indicated mild epithelial lesions (stellate), mild edema, stromal opacity, and a visible iris. A score of 2 indicated dendritic or atlas-like epithelial lesions covering <25% of the cornea, stromal edema with cloudy lesions covering <50% of the corneal diameter, and a visible iris. A score of 3 indicated epithelial lesions covering 25-50% of the cornea, stromal edema with cloudy lesions covering >50% of the corneal diameter, and a partially visible iris. A score of 4 indicated epithelial lesions covering >50% of the cornea, severe stromal edema, and opacity with a completely invisible iris.

From the second day post-infection onwards, a 0-4 grading scale (based on the proportion of the corneal area affected) was used as outlined by Trousdale et al. [17]: affected areas of <25%, ~50%, ~75%, and ~100% were allocated 1, 2, 3, and 4 points, respectively. Slit-lamp images were captured to record and assess keratitis severity for scoring.

Corneal thickness measurements

Central corneal thickness was measured using anterior segment OCT (RTVe XR 100, Opteva, Inc., Fremont, CA, USA) equipped with a specialized corneal adaptor lens (maximum scan depth and width of 2.4 and 8.0 mm, respectively). Sagittal cross-sectional images were acquired in crossline mode, and corneal thickness was determined using the ruler tool provided with the instrument.

Cell culture

Mouse-derived corneal stromal cells were isolated from the mouse cornea using dispase II (15 mg/mL) to separate the epithelium, followed by digestion with collagenase for 2 h. After obtaining the cell suspension, the cells were seeded in culture medium. The cells were cultured in DMEM/F12 medium (Gibco, USA) supplemented with 10% FBS (Gibco, USA) in a humidified incubator set at 37°C and 5% CO_2. For comparison, African green monkey kidney cells (Vero; ATCC, USA) were cultured under the same conditions.

Targeted PTGS2 signaling suppression

A PTGS2-targeting small interfering RNA (siRNA) (si-PTGS2, HY-RS11393) and a non-targeting control siRNA (si-NC) (both from MedChem Express) were used to suppress PTGS2 expression. The siRNA sequences used were as follows: siRNA-1: 5'-AGAAUGUGAUCAAGACUAAdTdT-3'; and siRNA-2: 1R: 5'-UAGCUCUGUCAUCAUCUCUdTdT-3', with 5'-GACGUAAACGGCCACAAGUTCdTdT-3', antisense 5'-ACUUGUGGCCGUUUACGUCGCdTdT-3' as the negative control siRNA sequence. Knockdown efficiency was assessed using quantitative Real-Time Polymerase Chain Reaction (RT-qPCR). All siRNAs were transfected into primary mouse corneal stromal cells for functional analysis (Supplementary Figure 1).

For siRNA transfection, primary mouse corneal stromal cells were cultured in 6-well plates until they reached 60-70% confluence. Transfection was performed using Lipofectamine™ 3000 (Invitrogen, USA), following the manufacturer's protocol. Briefly, siRNA was diluted in Opti-MEM medium (Gibco, USA) and mixed with Lipofectamine™ 3000 reagent. The siRNA-Lipofectamine™ 3000 complex was then added to the cells, and incubation was carried out for 6 hours at 37°C in a 5% CO_2 incubator. After the incubation period, the medium was replaced with fresh culture medium, and cells were allowed to grow for 24-48 hours before analysis.

Cell treatment

To explore the relationship between LUT and the NF-κB and PTGS2 inflammatory pathways, corneal stromal cells were first stimulated with 100 ng/mL Lipopolysaccharide (LPS) for 24 h to induce an inflammatory response. The cells were then treated with 20 μM LUT for an additional 24 h. Subsequently, the cells were cultured in 6-well plates, with the LPS-treated group serving as the control. The LUT treatment and control groups received 20 μM LUT dissolved in a culture medium and LPS alone, respectively.

RT-qPCR

Total RNA was extracted using an RNA extraction kit (TransGen Biotech, Beijing, China) and reverse-transcribed into complementary DNA (cDNA) with reverse transcriptase (Vazyme, Nanjing, China). Following that, qRT-PCR was performed using ChamQ Universal SYBR qPCR Master Mix (Vazyme) on an ABI Prism 7500 system (Applied Biosystems, Waltham, MA, USA), with β-actin serving as an internal reference. Relative gene expression levels were determined using the $2^{-\Delta\Delta Ct}$ method. The primer sequences used are detailed in Supplementary Table 4.

Western blot

A few infected animals were euthanized by cervical dislocation, and corneal tissues were subsequently collected on the third day post-infection, with three mice pooled to form one sample for further analysis. The collected corneal tissues were homogenized in ice-cold RIPA lysis buffer (Solarbio, Beijing, China) containing 1% Phenylmethylsulfonyl Fluoride (PMSF) and a phosphatase inhibitor cocktail (CWBio, Jiangsu, China). The homogenates were then incubated on ice for 30 min with a protease inhibitor (Beyotime Biotechnology) for complete protein extraction. Subsequently, the lysates were incubated with Sodium Dodecyl Sulfate-Polyacrylamide Gel Electrophoresis (SDS-PAGE) sample loading buffer (Beyotime Biotechnology) for 15 min at 98°C. After separation using SDS-PAGE (10% gel), proteins were transferred to Polyvinylidene Difluoride (PVDF) membranes (EMD Millipore, Billerica, MA, USA) via electroblotting.

Subsequently, the PVDF membranes were blocked with 5% fat-free milk dissolved in TBS/0.05% Tween-20 for 1 h at room temperature (RT). The membranes were then incubated with primary antibodies overnight at 4°C, followed by incubation with Horseradish Peroxidase (HRP)-conjugated goat anti-rabbit secondary antibodies. Protein bands were visualized and photographed using the ChemiDoc Touch System (Bio-Rad, Hercules, CA, USA) with ECL substrate (EMD Millipore). Protein expression levels were normalized across the samples using β-actin as a loading control. The protein bands were analyzed for relative quantification using Image J software. The antibodies used in the experiment are listed in Supplementary Table 5.

Statistical analysis

All statistical analyses were performed using GraphPad Prism 9. Data are expressed as

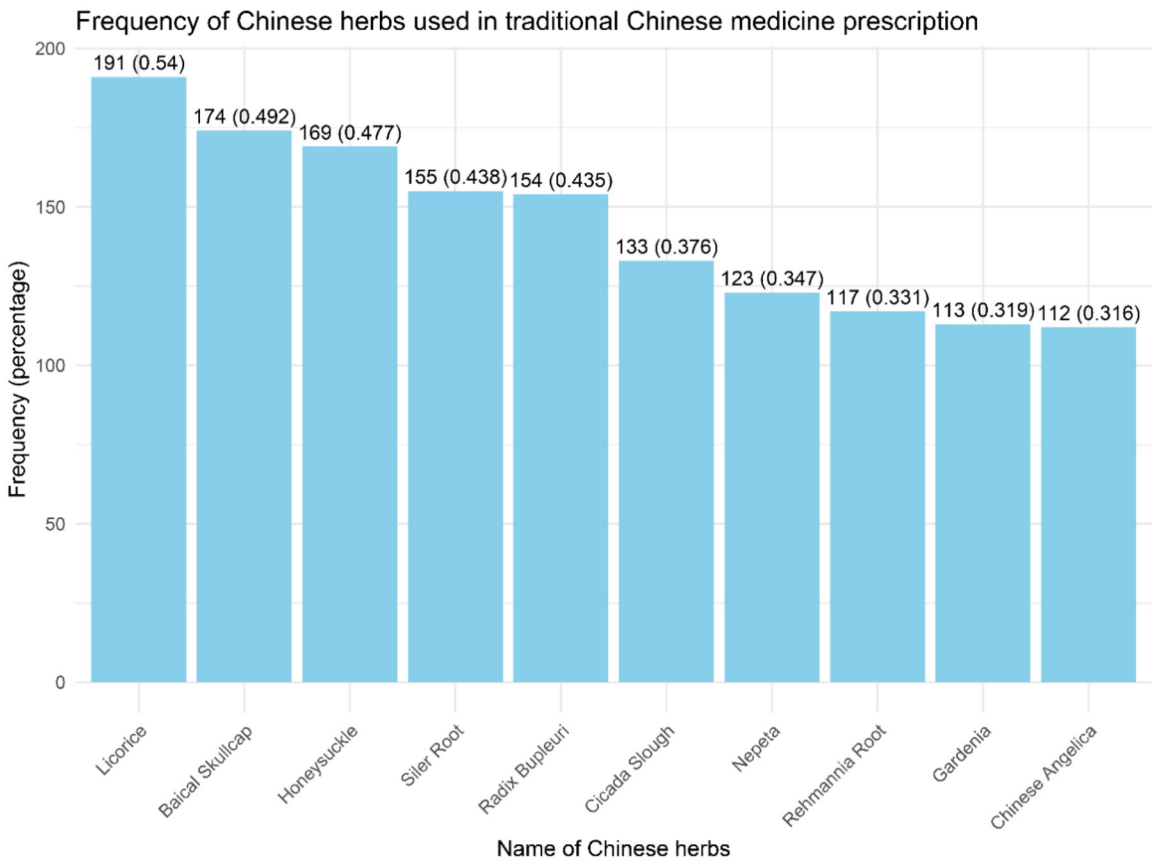

Figure 1. Frequency of Chinese herbs used in Traditional Chinese Medicine (TCM) prescription for Herpes Simplex Keratitis (HSK).

mean ± standard deviation (SD). For comparisons among multiple groups (three or more), one-way ANOVA was performed, followed by Bonferroni post-hoc correction for multiple comparisons. For experiments involving repeated measurements over time, repeated measures ANOVA was applied, with Bonferroni correction for post-hoc analysis to adjust for multiple comparisons. A p-value <0.05 was considered statistically significant.

Results

Profiling of core herbs, active ingredients, and latent target proteins in TCM prescriptions for HSK

Based on pre-established inclusion and exclusion criteria, we searched various databases for publications on TCM prescriptions for HSK, yielding 213 articles. From these articles, 354 TCM prescriptions were compiled, involving 165 different types of Chinese herbs. **Figure 1** shows the top 10 most frequent herbs, identified as core herbs in TCM prescriptions for HSK.

Among the 10 core herbs, 158 bioactive components with SMILES structures were identified (Supplementary Table 6). Based on these components, we created a "Herb-Potential Active Ingredient-Target" interaction network, comprising 210 target nodes and 9,930 edges (**Figure 2**). Furthermore, the GeneCards, DisGeNET, and OMIM databases were screened for HSK-related genes, yielding 544 target genes after deduplication, highlighting the complex mechanisms through which core herbs exert their effects in HSK treatment.

Core protein targets in TCM prescriptions for HSK

Among the 210 core herb targets and 544 HSK-related disease targets, 30 intersection genes were identified (**Figure 3A**). A PPI network encompassing 158 nodes was constructed using the STRING database (**Figure 3B**). The

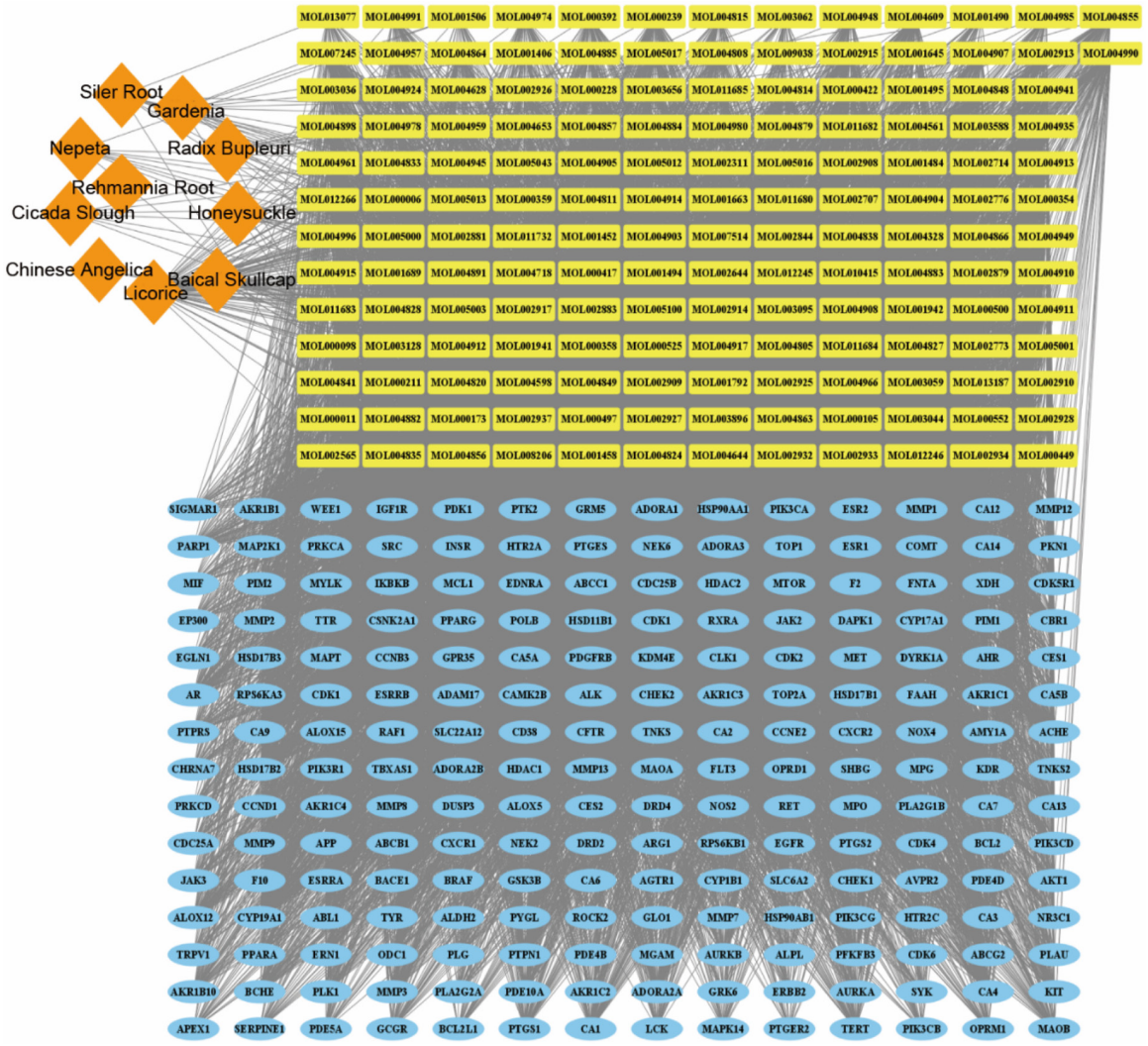

Figure 2. Relationship among TCM core herbs for HSK, active ingredients of herbs, and protein targets of active ingredients. Note: Orange indicates TCM core herbs for HSK; Yellow indicates active ingredients of herbs; Blue indicates protein targets of active ingredients.

nodes were screened based on their Degree Values (DVs). The top five protein targets were: AKT1 (DV=52), EGFR (DV=46), BCL2 (DV=44), PTGS2 (DV=42), and SRC (DV=38) (**Figure 3C**).

GO and KEGG enrichment analyses of core protein targets in TCM prescriptions for HSK

The 30 intersection target genes were subjected to GO analysis, yielding 637 terms with P<0.05. Among these, 566 BP-related terms were identified, with cell death regulation, stress response regulation, programmed cell death regulation, organic substance response, and apoptotic process regulation being the top five. Regarding CC-related terms, 29 items were identified, with the top five being external side of the membrane, vesicle lumen, lateral side of the membrane, cytoplasm, and cytoplasmic side of the plasma membrane. Finally, for MF-related terms, 42 entries were identified, with the top five being catalytic activity, acting on a protein, catalytic activity, protein kinase activity, and enzyme binding (**Figure 4A**).

In addition, we performed KEGG enrichment analysis, yielding 132 pathways associated with core drug interventions for HSK (P<0.05). These pathways were ranked by *P*-value, and the top 20 signaling pathways were selected for visualization (**Figure 4B**). The top 5 pathways

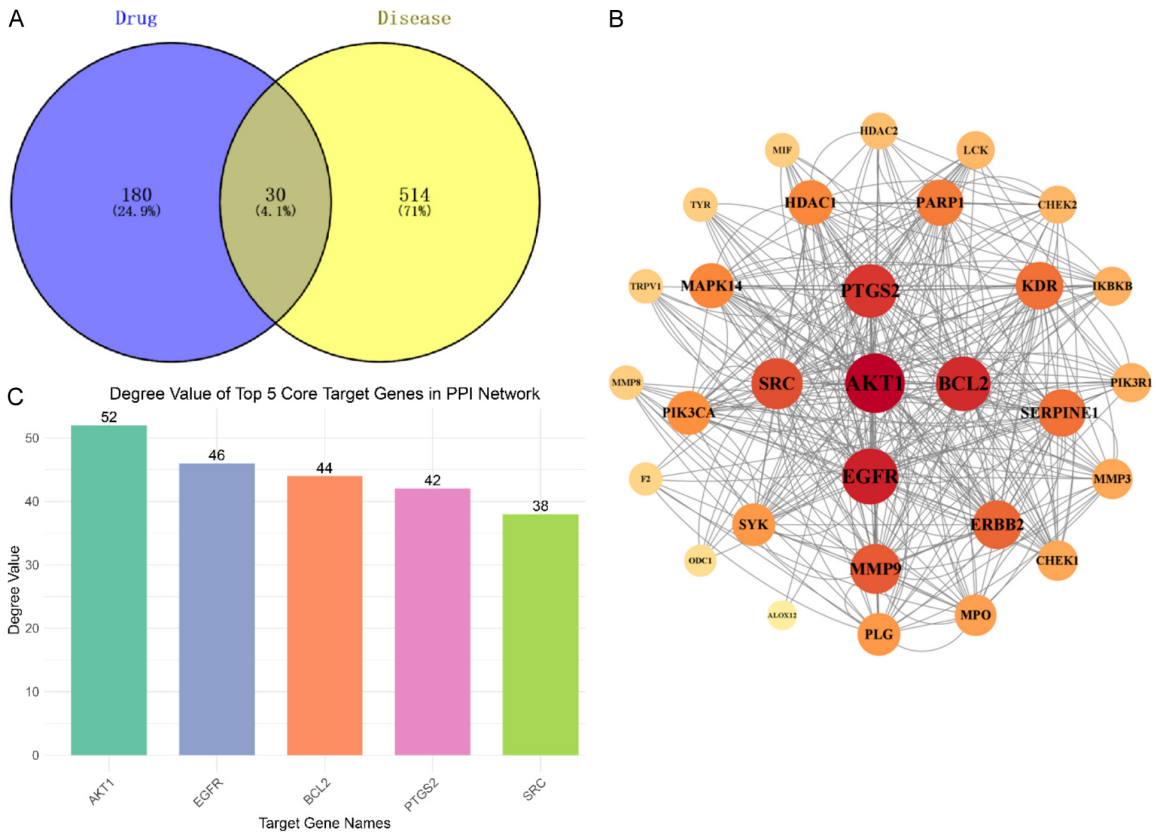

Figure 3. Core protein targets of TCM prescription for HSK. A: Venn Diagram of TCM core herb targets and HSK-related disease targets. B: Protein-protein interaction network (PPI) of 30 intersection target genes. C: Degree value of the top 5 core target genes in the PPI network.

included VEGF signaling pathway, EGFR tyrosine kinase inhibitor resistance, endocrine resistance, prostate cancer, PD-L1 expression, and PD-1 checkpoint pathway in cancer. Notably, the TNF signaling pathway, which was among the top 20 signaling pathways, has been intimately linked with PTGS2, one of the top five core targets [18, 19].

Optimum active ingredients of the TCM core herbs targeting the top 5 PPI core proteins: molecular docking analysis

The core proteins AKT1, EGFR, BCL2, PTGS2, and SRC, along with the active ingredients of TCM core herbs for HSK were subjected to molecular docking analysis to identify the optimum active ingredients that target these top 5 PPI core proteins. A binding energy of <-5.0 kcal/mol between the active components and core proteins indicates spontaneous binding, suggesting a strong interaction between the ligands and receptors. **Table 1** shows the active ingredients with the best binding capacity for the top 5 PPI core proteins. Specifically, PTGS2 exhibited the best binding capacity with LUT (binding energy =-9.7 kcal/mol). Meanwhile, the binding energies of Isolicoflavonol with EGFR, BCL2, SRC, and AKT1 were -7.6, -6.9, -5.6, and -9.1 kcal/mol, respectively (**Figure 5**). These findings suggest that LUT may interact closely with PTGS2 through the NF-κB signaling pathway, potentially playing a crucial role in modulating HSK.

LUT alleviated HSK in mice

Previous research has suggested that LUT can enhance type I interferon expression and activate the cGAS-STING signaling pathway, potentially inhibiting early HSV-1 infection in herpes simplex virus encephalitis [20]. In TCM prescriptions for HSK, common herbs like Honeysuckle (selected in 47.74% of prescriptions), Schizonepeta (selected in 34.75% of prescriptions), and Scutellaria (selected in 49.15% of

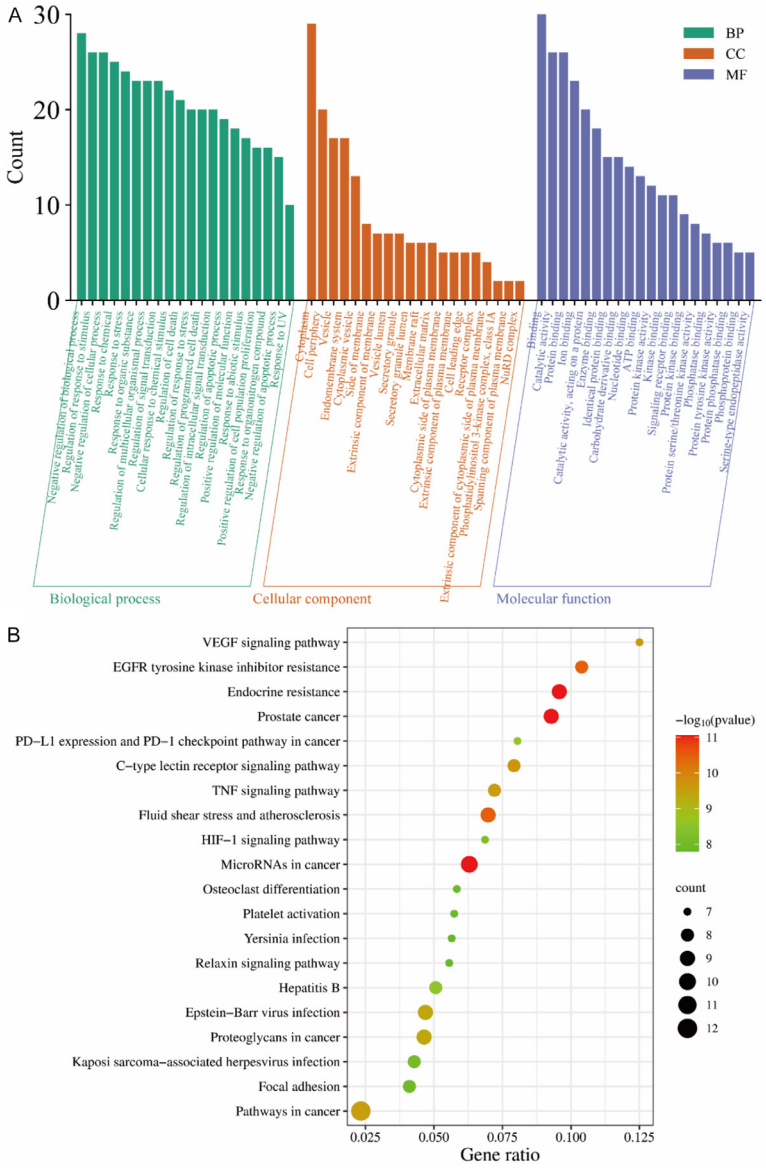

Figure 4. GO and KEGG functional enrichment analysis. A: GO Functional Enrichment Analysis. B: KEGG Functional Enrichment Analysis. Note: GO: gene ontology BP: Biological Process; CC: Cellular Component; MF: Molecular Function.

Table 1. Active ingredients of herbs with the best binding capacity for the top 5 PPI core proteins

Target protein	Best binding capacity	Binding energy (kcal/mol)
PTGS2	LUT	-9.7
AKT1	Isolicoflayonol	-9.1
EGFR	Isolicoflayonol	-7.6
BCL2	Isolicoflayonol	-6.9
SRC	Isolicoflayonol	-5.6

Note: PPI: Protien-protien interaction; AKT1: Serine/threonine-protein kinase; EGFR: Epidermal growth factor receptor; BCL2: B-cell lymphoma 2; PTGS2: Prostaglandin-endoperoxide synthase; SRC: Non-receptor tyrosine kinase.

prescriptions) are rich in LUT, implying that approximately 82.66% of the prescriptions contain LUT (Supplementary Table 6). However, the impact of LUT on HSK has yet to be fully reported.

To investigate this, HSK mouse models were treated with LUT eye drops to verify its effectiveness in alleviating HSK symptoms, revealing that the treatment significantly reduced corneal opacification (**Figure 6A**, **6B**) and corneal edema (**Figure 6C**, **6D**), with the overall injury alleviation increasing over time. These findings suggest that LUT plays a significant role in mitigating HSK-induced corneal damage.

LUT downregulated the NF-κB pathway, inflammatory responses, and HSK symptoms in mouse corneas

The NF-κB signaling pathway is a primary pathway activated when PTGS2 binds to its receptor PTGS2R [21]. Considering the significance of the NF-κB signaling pathway in keratitis [22], we further investigated LUT's effects on the NF-κB pathway and inflammatory responses in the corneas of HSK mice. Our results demonstrated a significant upregulation of the NF-κB pathway and inflammatory responses in the corneas of HSK mice (**Figure 7A**, **7B**).

We further downregulated the NF-κB pathway using BAY 11-7082 to confirm its role in HSK. Our findings revealed that NF-κB pathway downregulation significantly reduced corneal opacification (**Figure**

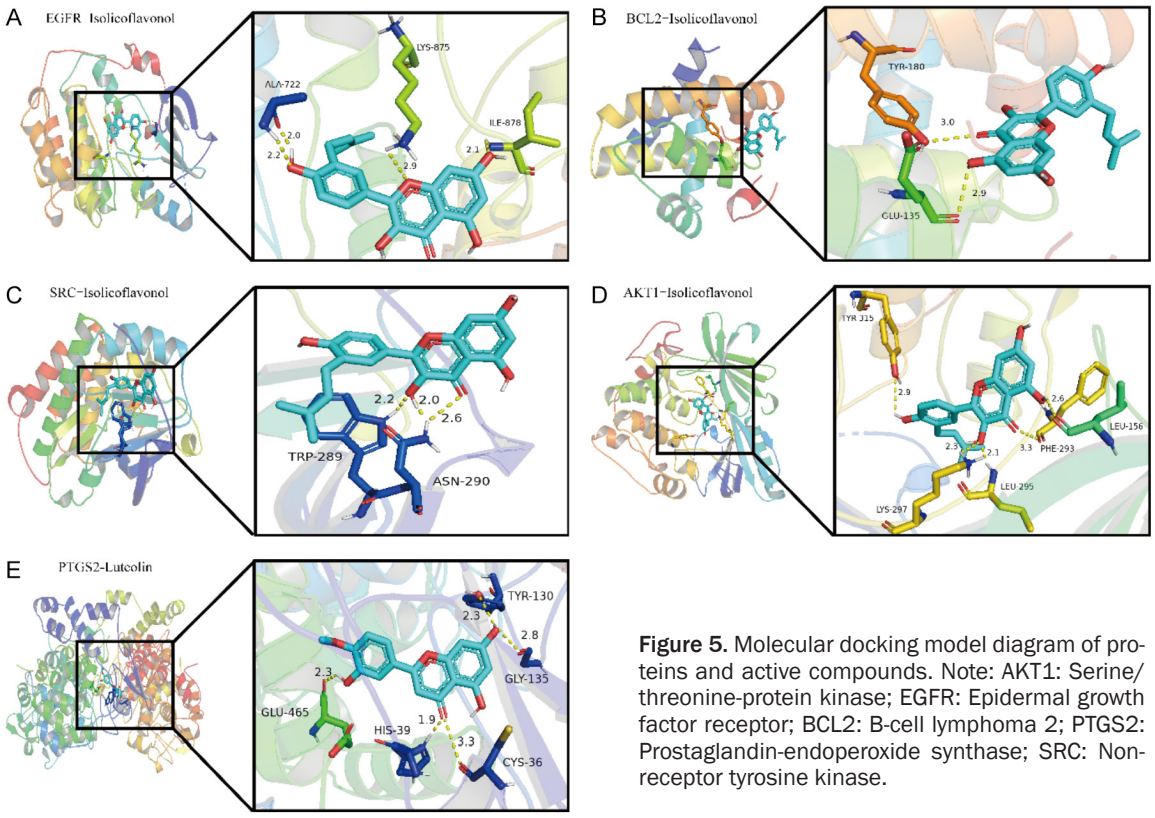

Figure 5. Molecular docking model diagram of proteins and active compounds. Note: AKT1: Serine/threonine-protein kinase; EGFR: Epidermal growth factor receptor; BCL2: B-cell lymphoma 2; PTGS2: Prostaglandin-endoperoxide synthase; SRC: Non-receptor tyrosine kinase.

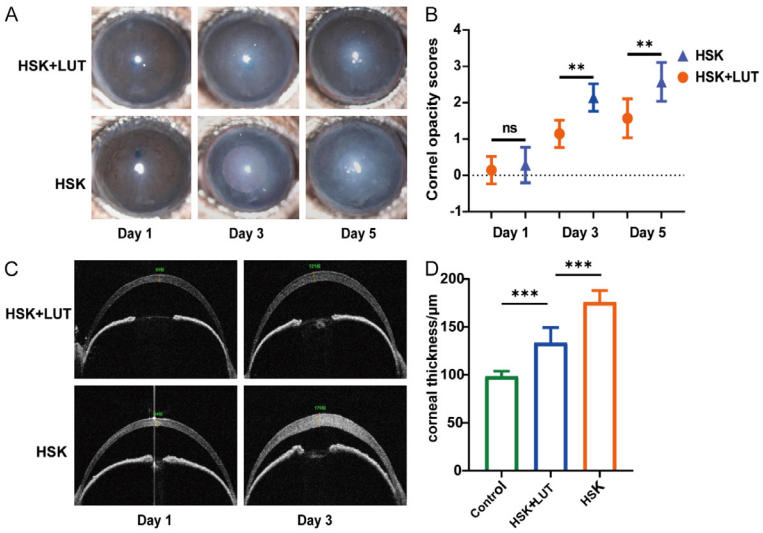

Figure 6. Luteolin (LUT) alleviated HSK in mice. A: Slit-lamp photographs showing corneal opacity over time in HSK and HSK+LUT groups; B: Comparison of corneal opacity scores between HSK and HSK+LUT groups at Day 1, 3, 5; C: Corneal thickness measured by RT-OCT; D: Corneal thickness measurement. ns: P>0.05; *, **: P<0.01; ***: P<0.001.

7C) and corneal edema (**Figure 7D**) in HSK mice cornea, implying that LUT effectively downregulates the NF-κB pathway and inflammatory responses to alleviate HSK.

Inhibition of PTGS2 downregulated the NF-κB pathway, inflammatory responses, and alleviated symptoms of HSK in the mouse cornea

To further investigate the role of PTGS2 in LUT's ameliorative effects on HSK, we first detected PTGS2 expression in the corneas of HSK mice with or without LUT treatment. The results revealed that LUT significantly downregulated PTGS2 expression in HSK mouse corneas (**Figure 8A**). We then knocked down PTGS2 in primary mouse corneal stromal cells and examined the NF-κB pathway. PTGS2 knockdown led to a downregulation of the NF-κB pathway (**Figure 8B**). Subsequently, we inhibited PTGS2 expression in the HSK mouse model using a PTGS2 inhibitor and treated the mice with LUT. Following PTGS2 inhibition, corneal inflammation was reduced, and HSK

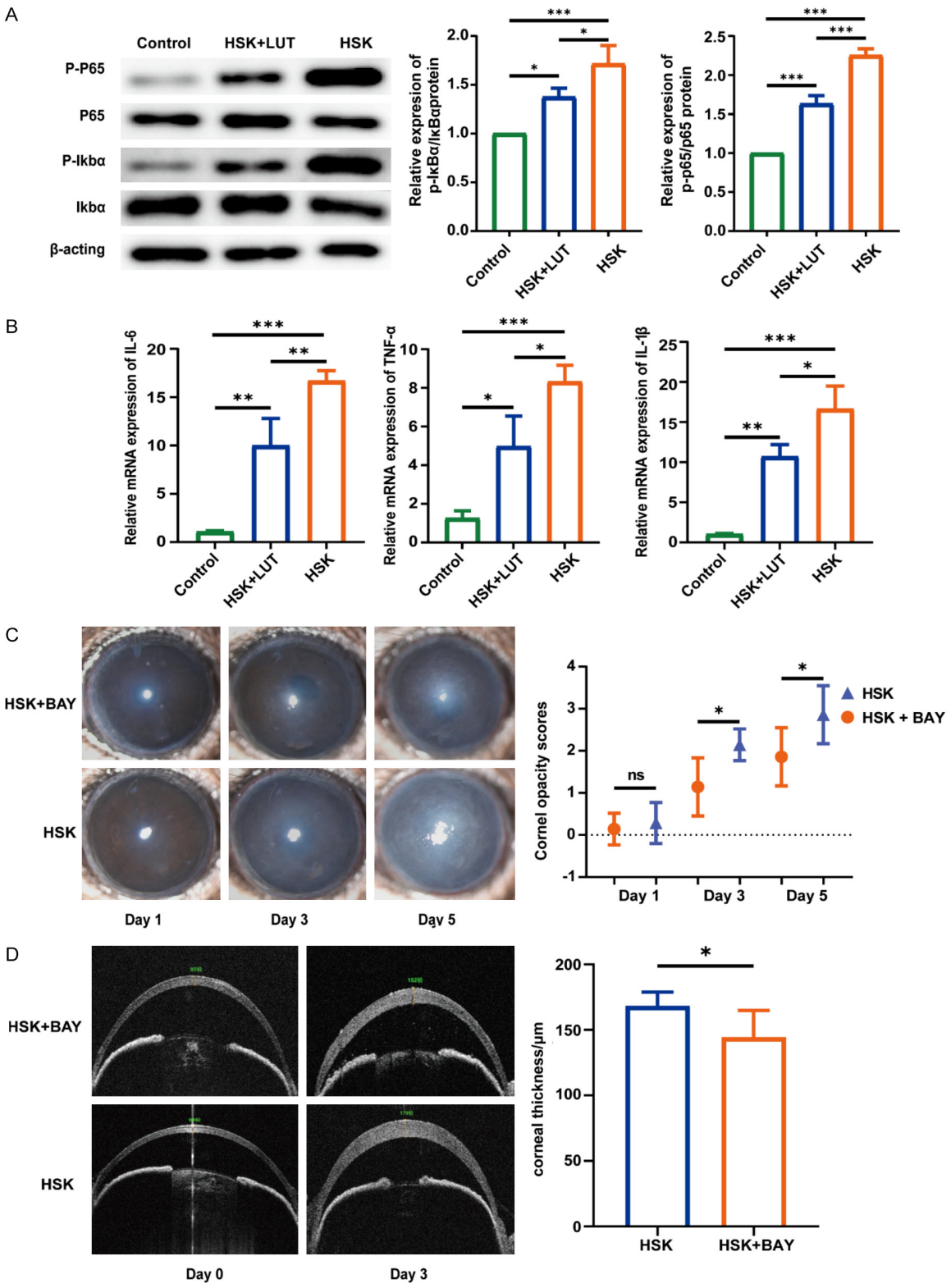

Figure 7. LUT alleviated HSK by suppressing NF-κB signaling and inflammatory responses in mouse cornea. A: The expression of NF-κB pathway proteins was significantly decreased in corneal tissues following LUT treatment, as assessed by western blotting. HSK+LUT: Group treated with LUT. Protein levels were normalized to β-actin (n=3). B: RT-qPCR results of inflammatory factors. C: Slit-lamp photographs and corresponding clinical scoring. HSK+BAY: Group treated with Bay inhibitor. D: RT-OCT and corneal thickness measurement. Data are presented as mean ± SD (n=3). ns: P>0.05; *: P<0.05; **: P<0.01; ***: P<0.001.

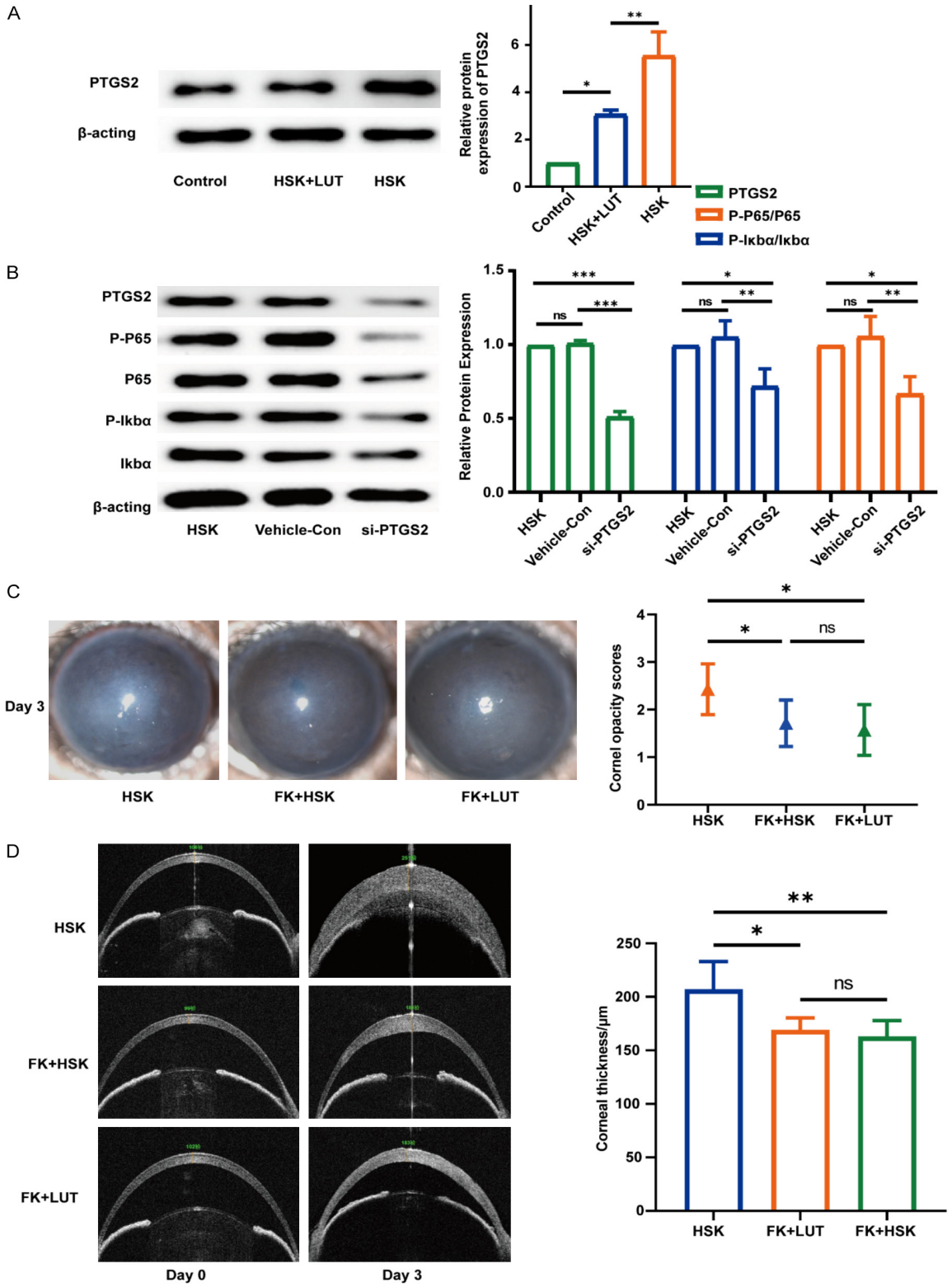

Figure 8. LUT alleviated HSK through PTGS2/ NF-κB pathway. A: Western blot analysis of PTGS2 expression in animal model treated with LUT. B: Western blot analysis of NF-κB pathway in cells with PTGS2 silencing by siRNA. Vehicle-Con: Control group treated with vehicle. si-PTGS2: cells treated with PTGS2-targeting siRNA. C: Slit-lamp photograph showing corneal condition under different treatment groups. FK+HSK: Group treated with FK inhibitor; FK+LUT: Group treated with FK inhibitor and LUT treatment. D: RT-OCT and corneal thickness measurement. ns: P>0.05; *: P<0.05; **: P<0.01; ***: P<0.001.

symptoms were alleviated. However, LUT treatment demonstrated a reduced efficacy in alleviating symptoms after PTGS2 inhibition (**Figure 8C**, **8D**).

LUT alleviated HSK by downregulating PTGS2 and inhibiting the NF-κB pathway

To further investigate the effect of LUT on the expression PTGS2 and the NF-κB pathway, we performed Western blot (WB) analysis. The results indicated that LUT treatment effectively downregulated PTGS2 expression and inhibited the phosphorylation of key NF-κB signaling proteins, including p-IκBα and p-p65 (Supplementary Figure 2). These findings suggest that LUT alleviated HSK by downregulating both PTGS2 and the NF-κB pathways, thus modulating inflammation in corneal stromal cells.

Discussion

The pathogenesis of Herpes Simplex Keratitis (HSK) is characterized by a complex interplay between the virus and the host's immune response [23]. While the host's immune reaction plays a critical role in clearing active HSV post-infection, it simultaneously triggers corneal inflammation responses that can lead to complications such as neovascularization and scarring [24]. Herein, we found that Luteolin (LUT), a major active component in TCM prescriptions, can modulate inflammatory and antiviral responses by inhibiting the PTGS2/NF-κB pathway, effectively alleviating HSK. These findings align with previous research highlighting the anti-inflammatory and antiviral properties of LUT [25-27], and offer novel insights into its mechanism of action in HSK treatment.

Beyond direct HSV-1 infection, the early pathological progression of HSK can also be attributed to an overactivated host immune response. Even when the viral load is controlled, the persistent release of inflammatory cytokines, along with aberrant neutrophil and Th17 cell infiltration, can culminate in corneal stromal lysis and neovascularization [28, 29]. These findings emphasize the significance of mitigating inflammation during the early stages of HSK [30]. Anti-inflammatory treatments, such as IFN-γ-induced therapy, have been shown to significantly reduce Th17 cell activation and IL-17-mediated inflammatory responses, alleviating early symptoms of HSK [31]. Through network pharmacology, we identified key targets involved in TCM-mediated HSK treatment. Our results suggest that these effective targets were primarily focused on combating inflammatory responses, a phenomenon that aligns with the current mainstream approach of controlling inflammation in the early stages of HSK. Therefore, we propose that the efficacy of traditional medicines in treating HSK is largely attributed to their ability to inhibit early-stage inflammation.

Our findings indicate that early inhibition of both the NF-κB pathway and PTGS2 significantly reduced the inflammatory response and clinical manifestations of early-stage HSK. The NF-κB pathway, a central hub for inflammation regulation, is rapidly activated through Pattern Recognition Receptors (PRRs), such as TLR7/MyD88, following HSV-1 infection [31]. This activation triggers the release of pro-inflammatory cytokines, such as IL-6 and TNF-α, which contribute to corneal stromal edema, neovascularization, and scarring [32]. Song et al. [33] reported that NF-κB inhibition alleviated HSV-1-induced microglial inflammation and herpes simplex encephalitis. Furthermore, Kui et al. [34] demonstrated that p38 inhibitors could block NF-κB phosphorylation, reducing CXCL10 secretion in HSV-1-infected corneal cells. Meanwhile, Jiang et al. [35] noted that NLRP12 overexpression suppressed IKKβ activity, thereby reducing neutrophil infiltration in the corneal stroma. Based on these insights, we speculated that the NF-κB pathway may be a key target in HSK treatment. Therefore, early inhibition of its activation, along with PTGS2 suppression, could serve as a viable strategy for controlling excessive inflammation and preventing corneal damage in HSK.

The anti-inflammatory and antiviral properties of LUT are well documented [36-38]. Ye et al. [39] reported that modified LUT effectively suppressed the NF-κB pathway, thus inhibiting the production of pro-inflammatory cytokines such as IL-1β and IL-6 in LPS-induced RAW cells. Similarly, Liu et al. [40] reported that Paeoniflorin+LUT downregulated the NF-κB signaling pathway, thereby alleviating inflammation in an Acute Lung Injury (ALI) mouse model. Beyond its anti-inflammatory effects, LUT also exhibits antiviral activity. Wang et al. [20] reported that LUT upregulated Type I interferons (IFN-α and

IFN-β), inhibiting the early stages of HSV-1 infection. Herein, we observed that LUT effectively downregulated key inflammatory mediators such as IL-1β, TNF-α, and IL-6 in HSK. Specifically, LUT reduced the phosphorylation levels of key NF-κB pathway proteins like p65 and IκBα, thereby inhibiting the subsequent inflammatory cascade. This ultimately mitigated HSK-associated tissue damage, underscoring LUT's critical role in inflammatory pathways, particularly in HSK.

Despite its valuable insights regarding LUT's therapeutic potential in HSK, this study still has several notable limitations. First, while the network pharmacology-based screening approach effectively identified potential active compounds, it is inherently limited by the accuracy and completeness in current databases. Second, TCM formulations typically involve complex mixtures of ingredients, with LUT being just one active component. The interaction between these compounds could lead to different dynamic effects on various signaling pathways. Consequently, to fully understand the therapeutic potential of TCM in managing HSK, future studies should explore LUT's broader immunomodulatory effects in the context of TCM, particularly how its effects may vary in combination with other active ingredients. Additionally, clinical data supporting the efficacy of LUT in treating HSK remain limited, necessitating additional, more robust clinical trials to validate its therapeutic potential. Future studies should focus on elucidating LUT's antiviral activity, particularly its ability to control HSV-1 replication and its effects on recurrent HSK. Understanding LUT's interaction with viral mechanisms and its potential role in preventing HSK recurrence would be crucial for assessing its long-term therapeutic value.

Overall, LUT may hold clinical promise in targeted therapeutic strategies for HSK, particularly in controlling inflammation-induced corneal damage while preserving antiviral defenses, although further validation is required. Our findings also provide valuable insights into the broader application of natural compounds in treating ocular inflammatory diseases.

Conclusion

This study demonstrates that LUT can alleviate HSK via downregulating the PTGS2/NF-κB pathway. LUT exerts anti-inflammatory effects in HSK treatment, highlighting the potential of TCM compounds in modern therapeutic approaches for ocular infections. Moreover, our findings pave the way for further research into the development of integrative treatments that leverage traditional and contemporary medical practices to manage infectious diseases such as HSK.

Acknowledgements

All authors are thankful for the grants from the National Natural Science Foundation of China (Grant No. 82171027) and Taishan Scholar Program (Grant No. ts20190983).

Disclosure of conflict of interest

None.

Address correspondence to: Yusen Huang, Shandong Eye Institute, #5 Yan'erdao Road, Qingdao 266071, Shandong, China. E-mail: huang_yusen@126.com

References

[1] Suvas PK, Setia M, Rana M, Chakraborty A and Suvas S. Novel characterization of CXCR4 expressing cells in uninfected and herpes simplex virus-1 infected corneas. Ocul Surf 2023; 28: 99-107.

[2] Zhu S and Viejo-Borbolla A. Pathogenesis and virulence of herpes simplex virus. Virulence 2021; 12: 2670-2702.

[3] Sibley D and Larkin DFP. Update on Herpes simplex keratitis management. Eye (Lond) 2020; 34: 2219-2226.

[4] Harris KD. Herpes Simplex Virus Keratitis. Home Healthc Now 2019; 37: 281-284.

[5] Foster A. Case study: clinical research. Community Eye Health 2022; 35: 4.

[6] Rowe AM, St Leger AJ, Jeon S, Dhaliwal DK, Knickelbein JE and Hendricks RL. Herpes keratitis. Prog Retin Eye Res 2013; 32: 88-101.

[7] Schalkwijk HH, Snoeck R and Andrei G. Acyclovir resistance in herpes simplex viruses: prevalence and therapeutic alternatives. Biochem Pharmacol 2022; 206: 115322.

[8] Robinet-Perrin A, Tumiotto C, Cornut T, Santoni A, Touboul D, Goupil-Gouyette T, Garrigue I, Boutolleau D and Burrel S. Input of recombinant phenotyping for the characterization of a novel acyclovir-resistance mutation identified in a patient with recurrent herpetic keratitis. Antiviral Res 2019; 168: 183-186.

[9] Musa M, Enaholo E, Aluyi-Osa G, Atuanya GN, Spadea L, Salati C and Zeppieri M. Herpes sim-

plex keratitis: a brief clinical overview. World J Virol 2024; 13: 89934.
[10] Yin J, Huang Z, Xia Y, Ma F, Zhang LJ, Ma HH and Li Wang L. Lornoxicam suppresses recurrent herpetic stromal keratitis through downregulation of nuclear factor-kappaB: an experimental study in mice. Mol Vis 2009; 15: 1252-1259.
[11] Li J, Jiang M, Yu Z, Xiong C, Pan J, Cai Z, Xu N, Zhou X, Huang Y and Yang Z. Artemisinin relieves osteoarthritis by activating mitochondrial autophagy through reducing TNFSF11 expression and inhibiting PI3K/AKT/mTOR signaling in cartilage. Cell Mol Biol Lett 2022; 27: 62.
[12] Di Petrillo A, Orrù G, Fais A and Fantini MC. Quercetin and its derivates as antiviral potentials: a comprehensive review. Phytother Res 2022; 36: 266-278.
[13] Li B, Du P, Du Y, Zhao D, Cai Y, Yang Q and Guo Z. Luteolin alleviates inflammation and modulates gut microbiota in ulcerative colitis rats. Life Sci 2021; 269: 119008.
[14] Xue L, Jin X, Ji T, Li R, Zhuge X, Xu F, Quan Z, Tong H and Yu W. Luteolin ameliorates DSS-induced colitis in mice via suppressing macrophage activation and chemotaxis. Int Immunopharmacol 2023; 124: 110996.
[15] Gendrisch F, Esser PR, Schempp CM and Wölfle U. Luteolin as a modulator of skin aging and inflammation. Biofactors 2021; 47: 170-180.
[16] Montgomery ML, Callegan MC, Fuller KK and Carr DJJ. Ocular glands become infected secondarily to infectious keratitis and play a role in corneal resistance to infection. J Virol 2019; 93: e00314-19.
[17] Trousdale MD, Nesburn AB, Su TL, Lopez C, Watanabe KA and Fox JJ. Activity of 1-(2'-fluoro-2'-deoxy-beta-D-arabinofuranosyl)thymine against herpes simplex virus in cell cultures and rabbit eyes. Antimicrob Agents Chemother 1983; 23: 808-813.
[18] Xu H, Wang H, Ning X, Xu Z and Zhang G. Integrated bioinformatics and validation reveal PTGS2 and its related molecules to alleviate TNF-α-induced endothelial senescence. In Vitro Cell Dev Biol Anim 2024; 60: 888-902.
[19] Tan C, Liu L, Liu X, Qi L, Wang W, Zhao G, Wang L and Dai Y. Activation of PTGS2/NF-κB signaling pathway enhances radiation resistance of glioma. Cancer Med 2019; 8: 1175-1185.
[20] Wang Y, Li F, Wang Z, Song X, Ren Z, Wang X, Wang Y and Zheng K. Luteolin inhibits herpes simplex virus 1 infection by activating cyclic guanosine monophosphate-adenosine monophosphate synthase-mediated antiviral innate immunity. Phytomedicine 2023; 120: 155020.
[21] Nam YW, Shin JH, Kim S, Hwang CH, Lee CS, Hwang G, Kim HR, Roe JS and Song J. EGFR inhibits TNF-α-mediated pathway by phosphorylating TNFR1 at tyrosine 360 and 401. Cell Death Differ 2024; 31: 1318-1332.
[22] Tang H, Huang L and Hu J. Inhibition of the m6A methyltransferase METTL3 attenuates the inflammatory response in fusarium solani-induced keratitis via the NF-κB signaling pathway. Invest Ophthalmol Vis Sci 2022; 63: 2.
[23] Chodosh J and Ung L. Adoption of innovation in Herpes Simplex Virus Keratitis. Cornea 2020; 39 Suppl 1: S7-S18.
[24] Shen W, Wang C, Jiang J, He Y, Liang Q and Hu K. Targeted delivery of herpes simplex virus glycoprotein D to CD169(+) macrophages using ganglioside liposomes alleviates herpes simplex keratitis in mice. J Control Release 2024; 365: 208-218.
[25] Wang J, Zeng X, Gou J, Zhu X, Yin D, Yin L, Shen X, Dai Y and Pan X. Antiviral activity of luteolin against porcine epidemic diarrhea virus in silico and in vitro. BMC Vet Res 2024; 20: 288.
[26] Caporali S, De Stefano A, Calabrese C, Giovannelli A, Pieri M, Savini I, Tesauro M, Bernardini S, Minieri M and Terrinoni A. Anti-inflammatory and active biological properties of the plant-derived bioactive compounds luteolin and luteolin 7-glucoside. Nutrients 2022; 14: 1155.
[27] Conti P, Caraffa A, Gallenga CE, Ross R, Kritas SK, Frydas I, Younes A, Di Emidio P, Ronconi G and Pandolfi F. Powerful anti-inflammatory action of luteolin: potential increase with IL-38. Biofactors 2021; 47: 165-169.
[28] Labib BA and Chigbu DI. Clinical management of Herpes Simplex Virus Keratitis. Diagnostics (Basel) 2022; 12: 2368.
[29] Lobo AM, Agelidis AM and Shukla D. Pathogenesis of herpes simplex keratitis: the host cell response and ocular surface sequelae to infection and inflammation. Ocul Surf 2019; 17: 40-49.
[30] Azher TN, Yin XT and Stuart PM. Understanding the role of chemokines and cytokines in experimental models of Herpes Simplex Keratitis. J Immunol Res 2017; 2017: 7261980.
[31] Koujah L, Suryawanshi RK and Shukla D. Pathological processes activated by herpes simplex virus-1 (HSV-1) infection in the cornea. Cell Mol Life Sci 2019; 76: 405-419.
[32] Wang L, Wang R, Xu C and Zhou H. Pathogenesis of Herpes Stromal Keratitis: immune inflammatory response mediated by inflammatory regulators. Front Immunol 2020; 11: 766.
[33] Song X, Cao W, Wang Z, Li F, Xiao J, Zeng Q, Wang Y, Li S, Ye C, Wang Y and Zheng K. Nicotinamide n-oxide attenuates HSV-1-induced microglial inflammation through sirtuin-1/NF-κB signaling. Int J Mol Sci 2022; 23: 16085.
[34] Xian-Kui H, Hui-Fang W, Jing-Ran S, Yu-Rong H, Bo-Yu C and Xiu-Jun S. P38 inhibition prevents Herpes Simplex Virus type 1 (hsv-1) infection

in cultured corneal keratocytes. Curr Eye Res 2020; 45: 1342-1351.
[35] Jiang J, Shen W, He Y, Liu J, Ouyang J, Zhang C and Hu K. Overexpression of NLRP12 enhances antiviral immunity and alleviates herpes simplex keratitis via pyroptosis/IL-18/IFN-gamma signaling. Int Immunopharmacol 2024; 137: 112428.
[36] De Stefano A, Caporali S, Di Daniele N, Rovella V, Cardillo C, Schinzari F, Minieri M, Pieri M, Candi E, Bernardini S, Tesauro M and Terrinoni A. Anti-inflammatory and proliferative properties of luteolin-7-O-glucoside. Int J Mol Sci 2021; 22: 1321.
[37] Shen R, Ma L and Zheng Y. Anti-inflammatory effects of luteolin on acute gouty arthritis rats via TLR/MyD88/NF-κB pathway. Zhong Nan Da Xue Xue Bao Yi Xue Ban 2020; 45: 115-122.
[38] Men X, Li S, Cai X, Fu L, Shao Y and Zhu Y. Antiviral activity of luteolin against pseudorabies virus in vitro and in vivo. Animals (Basel) 2023; 13: 761.
[39] Ye L, Xin Y, Wu ZY, Sun HJ, Huang DJ and Sun ZQ. A newly synthesized flavone from luteolin escapes from COMT-catalyzed methylation and inhibits lipopolysaccharide-induced inflammation in RAW264.7 macrophages via JNK, p38 and NF-κB signaling pathways. J Microbiol Biotechnol 2022; 32: 15-26.
[40] Liu Z, Gao J, Ban Y, Wan TT, Song W, Zhao W and Teng Y. Synergistic effect of paeoniflorin combined with luteolin in alleviating Lipopolysaccharides-induced acute lung injury. J Ethnopharmacol 2024; 327: 118022.

Supplementary Table 1. Information on databases and software used in the experiment

Databases	Software
China National Knowledge Infrastructure	DISGENET
Wanfang database	Pymol
TCMSP	Autodock tool
PubChem	STRING
Swiss Target Prediction	Venny

Supplementary Table 2. Selection criteria for literature

Inclusion criteria	Exclusion criteria
Patients with herpes simplex keratitis	Same prescription composition
Oral traditional Chinese medicine treatment	Animal experimental research
No corresponding complications	Nursing, case study, review, personal experience
Complete prescription of traditional Chinese medicine	
The treatment has statistical significance (P<0.05)	

Supplementary Table 3. Molecular docking procedure steps

Step	Content	Tools
1	Download the core protein structure, preprocess (remove water molecules, add charges, add hydrogens)	RCSB PDB AutoDock Tools
2	Download the ligand structure, preprocess	PubChem, Open Babel, AutoDock Tools
3	Determine the active site, perform molecular docking, calculate the binding score, and conduct visualization analysis	AutoDock Vina Pymol

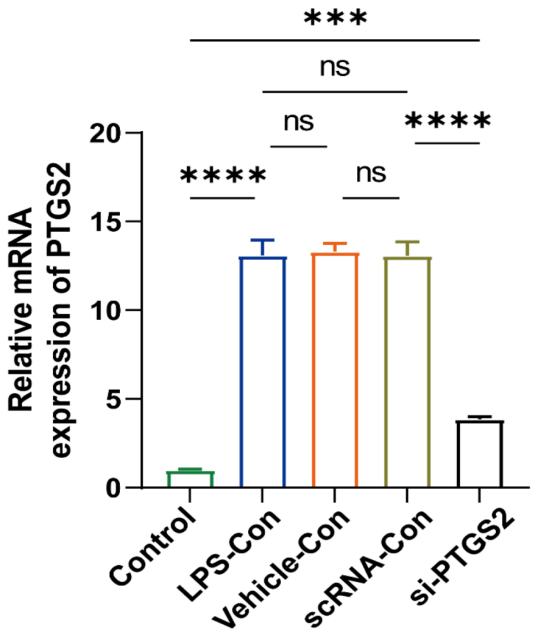

Supplementary Figure 1. Evaluation of PTGS2 knockdown efficiency. Control: untreated cells; LPS-Con: cells treated with LPS only (lipopolysaccharide-induced inflammation model); Vehicle-Con: cells treated with LPS and siRNA transfection reagent only; scRNA-Con: cells treated with LPS and scrambled siRNA; si-PTGS2: cells treated with LPS and PTGS2-targeting siRNA. ns: P>0.05; ***: P<0.001.

Supplementary Table 4. Primer sequences in RT-qPCR

Genes	Forward primer (5'-3')	Reverse primer (5'-3')
TNF-α	TGATGACATCAAGAAGGTGGTGAAG	TCCTTGGAGGCCATGTGGGCCAT
IL-1β	GAAATGCCACCTTTTGACAGTG	TGGATGCTCTCATCAGGACAG
IL-6	TAGTCCTTCCTACCCCAATTTCC	TTGGTCCTTAGCCACTCCTTC
PTGS2	ATGCTCGCCCGCGCCCTGCTGCTGT	TACGAGCGGGCGCGGGACGACGACA
β-actin	GGCTGTATTCCCCTCCATCG	CCAGTTGGTAACAATGCCATGT

Supplementary Table 5. Antibodies used in western blot

Target Protein	Antibody Name	Host Species	Dilution Ratio	Catalog Number	Manufacturer
Phospho-NF-κB p65	Anti-NF-κB p65 (phospho S536) Antibody	Rabbit	1:1000	ab76302	Abcam
Phospho-IKB alpha	Anti-IKB alpha (phospho S36) Antibody	Rabbit	1:1000	ab133462	Abcam
NF-κB p65	Anti-NF-κB p65 antibody	Rabbit	1:1000	ab32536	Abcam
IkB alpha	Anti-IkB alpha antibody	Rabbit	1:1000	ab76429	Abcam
COX2/Cyclooxygenase 2	Anti-COX2/Cyclooxygenase 2 Antibody	Rabbit	1:1000	ab283574	Abcam
Beta Actin	Anti-beta Actin Antibody	Rabbit	1:3000	ab8226	Abcam

Supplementary Table 6. Frequency of medication use in traditional Chinese medicine treatment for HSK

No.	Chinese Herbal Medicine	Frequency (times)	No.	Chinese Herbal Medicine	Frequency (times)
1	Licorice	191	6	Cicada Slough	133
2	Baical Skullcap	174	7	Nepeta	123
3	Honeysuckle	169	8	Rehmannia Root	117
4	Siler Root	155	9	Gardenia	113
5	Radix Bupleuri	154	10	Chinese Angelica	112

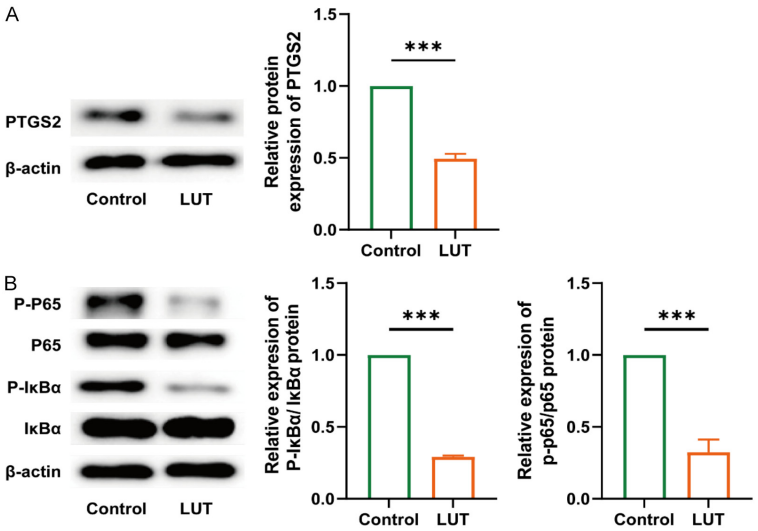

Supplementary Figure 2. LUT treatment reduces PTGS2 and NF-κB pathway activation. A. Western blot analysis of PTGS2 protein expression in the control and LUT-treated groups. The graph shows the relative protein expression of PTGS2 normalized to β-actin (n=3). B. Western blot analysis of NF-κB pathway proteins, including phosphorylated p65 (P-P65), total p65, phosphorylated IκBα (P-IκBα), and total IκBα in the control and LUT-treated groups. The graph shows the relative expression of P-IκBα/IκBα and P-p65/p65, normalized to β-actin (n=3). ***: P<0.001.